Beta2 oscillations in the hippocampal-cortical novelty detection circuit

Author list: Arthur S C França; Nils borgegius; Mike X Cohen;

Abstract

Novelty detection is a core feature of behavioral adaptation, and involves cascades of neuronal responses – from initial evaluation of the stimulus to the encoding of new representations – resulting in the behavioral ability to respond to an unexpected input (Kafkas and Montaldi, 2018; van Kesteren et al., 2012). In the past decade, a new important novelty detection feature, beta2 (~20 - 30 Hz) oscillations, has been described in the hippocampus (Berke et al., 2008; França et al., 2014; Kitanishi et al., 2015). However, the interactions between beta2 and the hippocampal network is unknown, as well as the role – or even the presence – of beta2 in other areas involved with novelty detection. We used behavioral tasks that modulate novelty in combination with multisite local field potential (LFP) recordings (acquired by custom-designed and self-made electrode arrays) targeting the CA1 region of the hippocampus, parietal cortex and mid-prefrontal cortex in mice, to describe the oscillatory dynamics among the regions involved with novelty detection processing. We found that transient beta2 power increases were observed only during interaction with novel contexts and objects, but not with familiar contexts and objects. Robust theta-gamma cross-frequency coupling was observed during exploration of novel environments. Surprisingly, bursts of beta2 power had strong coupling with the phase of delta-range oscillations. Finally, the parietal and mid-frontal cortices had strong coherence with the hippocampus in both theta and beta2 during novelty exploration. These results highlight the importance of beta2 oscillations in a larger hippocampal-cortical circuit, suggesting that beta2 is a mechanism for detecting and modulating behavioral adaptation to novelty.

1.0 - Introduction

Novelty detection is a crucial feature for behavioral adaptation and ignites cascades of neuronal responses, from the initial evaluation of the stimulus to the encoding of new representations, resulting in the behavioral ability to respond appropriately and adaptively to unexpected stimuli (Kafkas and Montaldi, 2018; van Kesteren et al., 2012). Over recent decades, an important novelty detection feature, beta2 oscillations (~20-33 Hz), has been described in the hippocampus (Berke et al., 2008; França et al., 2014; Kitanishi et al., 2015). In particular, beta2 power transiently increases during spatial novelty (Berke et al., 2008; França et al., 2014; Kitanishi et al., 2015) and its generation is implicated with AMPA and NMDA receptors plasticity between the connections of CA3 and CA1 hippocampal regions (Berke et al., 2008; Kitanishi et al., 2015). However, the interaction between beta2 with other hippocampal rhythms remains unknown. Furthermore, the hippocampus is not alone in detecting novelty: Evidence in both humans and rodents points to a larger hippocampal-cortical circuit for detecting and adapting to novelty, including the mid-prefrontal cortex (mPFC) and parietal cortex (PAR) (Kafkas and Montaldi, 2018; Pho et al., 2018; Spellman et al., 2015). It seems plausible that beta2 oscillations are a mechanism of communication across these regions, but there is currently no empirical evidence for or against this possibility.

Here we tested three novel hypotheses concerning the role of beta2 in novelty detection: First, beta2 power increase is associated with different forms of novelty (spatial and object); Second, slower oscillatory activity in the hippocampus modulates beta2, similar to gamma oscillations during memory encoding; Third, the novelty and familiarity integration hubs in the cortex synchronize with hippocampal beta2 oscillations during novelty exploration.

Through behavioral tasks that modulate novelty content exposed to the animal combined with local field potential (LFP) recordings acquired by custom-designed electrode arrays (Franca et al., 2020) targeting the CA1 region of the hippocampus (HC), PAR, and mPFC, we aimed to describe the interactions among these regions involved with novelty detection processing. Using weighted phase lag index (WPLI), Granger causality and cross-frequency phase-amplitude coupling (CFC) as indices of local and long-range synchronization (Canolty and Knight, 2010; Hyafil et al., 2015; Vinck et al., 2011), we found that transient beta2 power increases are observed only during interactions with novel contexts — environment or object — but not with familiar contexts. During novelty exploration, robust CFC was observed between theta and multiple gamma subbands. Unexpectedly, beta2 had robust coupling with delta-range oscillations. Finally, the PAR and mPFC cortices exhibited strong coherence with both theta and beta2 during novelty exploration, and exhibited a similar pattern of coupling as seen in the hippocampus. The results reported in the present study point to the direction of beta2 as an oscillatory feature independent of slow gamma oscillations, having the different dynamics of power and CFC, and connected to novelty detection. The synchronization among hippocampus, mPFC and PAR in beta2 during novelty detection reveals its characteristic as an important feature to understand novelty exploration and its implication in a broad hippocampal-cortical circuit for novelty detection.

2. 0 Methods

2.1 – Animals:

The data shown in this paper is from 9 animals with Black57 mice background. All animals were recorded in all sessions described in Figure 1A. The animals had free access to food and water. All experiments were approved by the Centrale Commissie Dierproeven (CCD) and it is according to all indications of the local Radboud University Medical Centre animal welfare body (Approval number 2016-0079).

2.2 – Electrode implant procedures:

The electrodes utilized in the present work were custom-designed and self-made electrode arrays to target three different regions of the mouse brain: HC, PAR and mPFC. A detailed description of the arrays and the manufacturing process can be verified at (Franca et al., 2020). There were 16 channels in mPFC, 8 channels in PAR, and 8 channels in HC.

10-16 week old mice were anesthetized with Isoflurane (induction at 5% Isoflurane in 0.5L/min O2; maintenance at 1-2% Isoflurane in 0.5L/min O2) [Teva]. For surgery, mice were fixed in the stereotaxic instrument [Neurostar Stereotaxic]. After shaving, the skin was disinfected with ethanol (70%). The local anesthetic Xylocaine (2%, Adrenaline 1:200.000 [AstraZeneca]) was injected subcutaneously at the incision site before exposing the skull. Peroxide (10~20% H2O2; [Sigma]) was applied to the skull with a cotton swab for cleaning and visualization of bregma and lambda. The windows in the skull through which the electrodes were lowered into the brain are drilled specifically to accommodate the type of arrays to be implanted. To avoid contact between the dental cement and the brain, vaseline was applied to the windows after the implant. Electrodes and screws were fixated onto the skull with dental cement (Super-Bond C&B) (Figure 2C). Approximately 40 minutes prior to the end of the surgery, saline and analgesic (Carprofen injected subcutaneous) were injected to facilitate recovery of the animal.

2.3 – Behavioral task

The experiments were designed to expose the animal to different hippocampus-dependent novelty content (environment and novel object), therefore no behavior performance output involving task was extracted or utilized in the analyses. The objective was to be able to evoke and investigate the novelty-related oscillatory features previously described. The experiment consisted of four main different sessions of 10 min recording - two sessions at Open Field and two sessions at Open Field with Objects - interspersed by 5 minutes Home Cage recordings (see Figure 1A).

2.4 – Electrophysiological analysis:

2.4.1 – Data inspection.

Electrophysiology data were acquired using Open Ephys with a sampling rate of 30 kHz. During preprocessing, data were down sampled to 1000 Hz, and EEGlab (Delorme et al., 2011) was used for

visual inspection and cleaning artifacts (open channels were removed from the analysis; high frequency noises were removed by Independent Component Analysis; Segments containing large deflections in all channels were used as a criteria for recording session exclusion). Six animals had high-quality data in all recording sessions, therefore statistical analysis concerning all sessions were performed in 6 animals. Analyses in different sessions therefore have a different number of animals (varying between 7 and 9).

2.4.2 – Data Analysis

The data analysis was performed using custom-written and built-in routines in Matlab (R2015b). Prior to analyses, the multichannel data from each region were re-referenced to that region's local average.

Spectral and time-frequency analysis was performed via convolution with complex Morlet wavelets (defined as a frequency-domain Gaussian with a 3 Hz full-width at half-maximum) that ranged in peak frequency from 2 Hz to 80 Hz in 100 linearly spaced steps. We reduced the dimensionality of the multichannel data by implementing a frequency-specific guided source-separation method based on generalized eigendecomposition. The goal was to create a linear weighted combination of channels (separately per region) that maximized the multivariate energy between the data covariance matrix from the narrowband filtered data, versus the broadband filtered data. This results in a single time series from each region, which was subjected to further analyses. We and others have shown that this method increases signal-to-noise characteristics while reducing computational costs and multiple-comparisons issues, and is more accurate than other source separation methods such as principal components analysis and independent components analysis (de Cheveigné and Arzounian, 2015; Cohen, 2017; Haufe et al., 2014). The Hilbert transform was then applied to these narrow-band filtered component time series in order to extract time-varying power and phase estimates.

The power spectrum was computed by averaging over the time-frequency power time series from all time points within each larger time window. Cross-frequency phase-amplitude coupling was performed in sliding windows of 5 seconds. The phase of delta and theta frequency (2-12Hz) and the amplitude of beta2 to mid-gamma (20 – 100 hz) was extracted. The raw CFC values were transformed into standard deviation (z) values by computing the normalized distance away from a null-hypothesis surrogate distribution, created by 500 permutations in which the phase angle time series were randomly cut and swapped. To decrease the influence of possible volume conduction we performed coherence computations utilizing weight-phase lag index (WPLI –(Vinck et al., 2011). Statistical analyses were performed using the routine RMAOV1 - Repeated Measures Single-Factor Analysis of Variance Test (alpha = 0.05).

Conditional spectral Granger causality was applied using the MultiVariate Granger Causality toolbox (Barnett and Seth, 2014). As this relies on the time-domain signals and not already-filtered data (because the causality spectrum is computed from the autoregression terms), we dimension-reduced each region using principal components analysis, taking the time series of the largest component from each region. Data were downsampled to 250 Hz and a model order ranging from 100-200 ms (varied over animals to best fit each dataset) was used for the autoregression model fitting. The advantage of the conditional

Granger analysis is that it allowed us to isolate the unique contributions of one region to a second region while accounting for possible shared variance with the third region.

3.0 - Results

3.1 - Beta2 power increases with both spatial and object novel content

We custom designed electrodes arrays of 32 channels for implant in the three different areas of interest: HC (8 channels), PAR (8 channels) and mPFC (16 channels - SuppFigure1). The behavioral experiments were designed to expose the animal to different hippocampus-dependent novelty contexts (environment and novel object), therefore no behavioral output involving task performance was required in the analyses. The experiment consisted of four sessions of successive 10 min recordings. Two sessions at Open Field (OF1 Novel; OF2 Familiar) and two sessions at Open Field with Objects (OBJ1 Novel; OBJ2 Familiar) - interspersed by 5 minutes Home Cage recordings (see Figure 1A). We extracted a single LFP component from each region using a frequency-specific multivariate source-separation method called generalized eigendecomposition (de Cheveigné and Arzounian, 2015; Cohen, 2017), which identifies a linear weighted combination of channels per region that maximizes a multivariate frequency-specific signal-to-noise ratio (details in Methods).

We first verified that both spatial and object novelty evoked the same pattern of power dynamics previously described (Berke et al., 2008; França et al., 2014). As expected, beta2 power increased only during novelty (OF1 and OBJ1, Figure 1B), but not during any of the familiar contexts (Home cage, OF2 and OBJ2, Figure 1B - Table 1). We also verified the transient novelty-related beta2, whereby the power returned to initial levels after around three minutes of novelty exposition (Figure 1C). For all further analyses, we utilized four time windows based on the power dynamics of beta2 in the HC verified during the exploration of novelty (Figure 1C). Power spectral density in the four time windows showed that beta2 power was higher in the first compared to the later time windows (Figure 1 D- Table 1).

3.2 - Delta modules beta2 amplitude during spatial and object novelty.

Given the role of CFC in the HC during spatial navigation, learning and memory retrieval, we explored whether CFC was modulated during novelty processing (using frequency ranges of 2-12 Hz for phase and 20-100 Hz for power). The open-field exploration does not present any well-defined time event to trigger time windows for the CFC, therefore we calculated the modulation index (MI) in sliding time windows, which allowed us to examine both the overall CFC and the temporal dynamics of CFC. We observed two key features of novelty-related CFC: First, we verified theta-gamma CFC for both low-gamma (30 - 50Hz lowG) and mid-gamma (60 - 80Hz midG); second, CFC was present between theta phase and beta2 power and between delta phase and beta2 and lowG power in the same time window of higher beta2 power (Figure 2A). A similar pattern of CFC was also observed in the first exploration of OBJ1 (Figure 2B).

Second, we verified the temporal dynamics of the most prominent CFC patterns: delta-beta2, delta-lowG, theta-beta2, theta-lowG and theta-midG. All the couplings were higher in the first time

window, suggesting that most part of novelty detection and encoding computation happened during the time window of strong beta2 power (Figure 2A and B - Table 2). During the re-exposition of the Open-Field and Object (OF2 and Obj. 2) we observed small or no changes in the dynamic of beta2 power (SuppFigure2 Table 4). However, all time-windows exhibit strong MI for delta-beta2/theta-beta2 and delta-LowG/theta-lowG for the OF2 session, and in the first time-window of OBJ2 session (SuppFigure2 Table 4).

3.3 - Novelty modulates oscillatory coherence in hippocampal-cortical circuitry.

Our third key hypothesis was that beta2 oscillations play an important role in the hippocampal-cortical novelty detection system. We therefore computed a measure of pairwise coherence (weighted phase-lag index, WPLI) between the three regions. This computation was performed in all recording sessions.

We observed theta-band coherence among all pairs of areas (see Figure 3A-C). Both types of novelty additionally exhibited coherence in beta2 range (Figure 3A-B). We also note that differently from the first Home exploration session, after being exposed to sessions of novelty content the animals exhibited higher coherence between HC and mPFC, and between HC and PAR, but not between the two cortical areas (Figure 3C). The bursts of Beta2 could be verified in the raw data in all regions analyzed (SuppFigure3 A and B), as also the independent bursts of beta2 and lowG (SuppFigure3 A).

We next applied conditional spectral Granger causality to determine the causal flow of interactions around this circuit. During the OF1, PAR and HC provided input into the mPFC in theta, beta2, and lowG ranges (Figure 3D). While in the Object1 session, PAR exhibited higher gain in the lowG frequency band (Figure 3E). HC dominated the gain values towards both cortices in both theta and Beta2 (Figure 3E).

3.4 - Parietal and mid-prefrontal cortices exhibit strong delta-beta2 coupling during novelty exploration.

Lastly, to further characterize the participation of PAR and mPFC cortices in processing novelty information, we verified both power and the coupling dynamics in the cortices during novelty detection exploration. The mPFC exhibited similar beta2 power dynamics as in the HC, where the increase of beta2 power was verified in the first time window. The power spectrum density (PSD) revealed an increase in beta2 frequency specifically during the novelty exploration (Figure 4A Table3). Such an increase in beta2 could be seen in the raw data, and was also independent from bursts in the HC (SuppFigure3).

Unexpectedly, the PAR and mPFC cortices not only exhibited strong coherence among each other and the HC, but also presented a similar pattern of coupling as seen in the HC (Figure 3A-C; Figure 4 Table 3), where the novel content induced strong modulation index (MI) between delta/beta2, theta/beta2, theta/lowG in the time-window 1. In the opposite, familiar sessions do not exhibit an increase in the delta/beta2 in any time window (SuppFigure2 B and C Table 4), in fact most of time windows analyzed did not present any coupling during the familiar session (SuppFigure2 B and C Table 4). These results

suggest that beta2 carries the novelty oscillatory feature and in the local network of each region beta2 is modulated in the same phase frequency.

4.0 – Discussion

For the first time, beta2 oscillations have been characterized in the hippocampal-cortical novelty detection circuit through simultaneous extracellular recordings of the HC CA1 region, PAR and mPFC of mice. We found that beta2 hippocampal power increases during both spatial and object novelty, but not during exploration of familiar contexts. We have shown that delta oscillations module beta2 and lowG during the exploration of new environments, while theta modules beta2 and lowG and midG. We found strong coherence in theta and beta2 bands during novelty exploration among the areas recorded, where the higher Granger gain for beta2 and theta came mostly from HC. Such coherence was translated into the increase of beta2 power in the mPFC. Finally we have described similar coupling characteristics in the cortex as was observed in the HC, showing that beta2 is also modulated by delta-band activity in the cortex. Taken together, these results highlight the importance of beta2 oscillations in a larger hippocampal-cortical circuit, suggesting that beta2 is a mechanism for detecting and modulating behavioral adaptation to novelty.

The three regions investigated in the present study, HC, PAR and mPFC, 1 - have monosynaptic connections among each other (Cenquizca and Swanson, 2007), 2 - are extensively related to learning and encoding of memory (Hasselmo, 2006; de Lima et al., 2011; Lisman and Grace, 2005; Lisman and Otmakhova, 2001, Preston and Eichenbaum, 2013; Sigurdsson et al., 2010; Spellman et al., 2015, Cross et al., 2013), a characteristic which is preceded by the novelty detection (van Kesteren et al., 2012) and 3 - are implicated in novelty detection networks in human models (Kafka and Motaldi, 2018). Here we collect LFP recordings from the HC, and PAR and mPFC cortices of the mice to verify if the functional connections previously described may form a network for novelty detection.

To coordinate the activity of such diverse brain areas during the process of novelty detection, oscillations would play a key role in the integration and coordination of the information (Buzsáki and Draguhn, 2004; Fries, 2005). Theta oscillations are thought to coordinate neural networks during memory encoding within and across different areas (Benchenane et al., 2011; Colgin, 2015; Tort et al., 2009). The close relationship between HC and mid-prefrontal areas as it relates to memory encoding and retrieval has been extensively reported (Benchenane et al., 2010, 2011; I.b.h, 2019), and theta plays an important role in mediating the function of these two areas (Benchenane et al., 2010, 2011). But until now, no specific oscillatory dynamic responsive to novelty content was reported playing a role in the coordination of different brain areas responsible to process the novelty information.

We and others have identified beta2 as an oscillatory feature in novelty detection in the HC (Berke et al., 2008; França et al., 2014; Kitanishi et al., 2015). This oscillation has a spectral peak around 20 to 30Hz in mice (Berke et al., 2008; França et al., 2014), and slightly faster in rats – 25 to 48Hz (Kitanishi et al., 2015). The beta2 is elicited with spatial/environmental novelty (Berke et al., 2008; França et al., 2014; Kitanishi et al., 2015), but not with olfactory novel stimulus (Berke et al., 2008). Beta2 also has transient characteristics, reaches the peak during the first 2 minutes after the novelty presentation and decrease with time (Berke et al., 2008; França et al., 2014), having the possible origin in the projections of CA3

towards CA1 (Berke et al., 2008; Kitanishi et al., 2015). Beta2 has been related to the stability of Place Fields (Berke et al., 2008; Kitanishi et al., 2015), memory consolidation impairment of novel recognition (França et al., 2014) and implicated to drive the synaptic delivery of GluR1-containing AMPA receptors (Kitanishi et al., 2015) and CA3 NMDA receptors (Berke et al., 2008;). Finally, beta2 has been reported absent in primary sensory and motor cortices (França et al., 2014), regions not associated with novelty detection (França et al., 2014).

In the present work we replicate the main features in the power dynamics reported before (Figure 1A-C, Table 1). Similarly to the previous reports, we have shown that beta2 can be verified at the raw signal of the HC channels (SuppFigure3). The results reported in the present work, in accordance with what has been previously described, shows a delay between the beginning the novelty exposition and the peak of beta2 (Figure 1C, Table 1), this latency period may reflect the generation of mismatch from previous expectations (Grossberg, 2009) or the time that animals take to perceive the experience as novel. One other possibility is the delay being related to the stability of the place field that is followed by the dynamic of beta2 (Berke et al, 2008).

The sliding time-window CFC analysis in the HC, especially during the first 150 seconds (window 1), revealed theta-nested spectral components, consistent with previous reports (Lopes-dos-Santos et al., 2018). The CFC revealed the peak of theta/beta2 around 22Hz (instead of the 25Hz of beta2 power increase – Figure 2A), Theta/lowG at 35Hz and theta/midG around 70Hz (Figure 2A) or 54Hz (Figure 2A). We observed an increase of coupling during the exploration of novel environment and objects (Figure 2A and B), while theta/lowG more prevalent in the "retrieval" at the familiar session (SuppFigure 2A Table4) accordingly to previously reported theta/midG coupling increases during learning and retrieval of memory (Lisman and Jensen, 2013; Lopes-dos-Santos et al., 2018; Tort et al., 2008, 2009; Zheng et al., 2016). Interestingly, beta2 and lowG were strongly modulated by the delta phase (Figure 2A and B). Although initially this could point to beta2 and lowG as being part of the same oscillatory regimen, beta2 and lowG have different spectral peaks (25Hz vs 35Hz), beta2 has a transient power characteristic and lowG does not (Figure 1 C, table 1) and inspecting the raw signal reveals that these two dynamics can be observed independently of each other (SuppFigure 3A). Furthermore, beta2 and lowG have different coherence peaks (Figure 3), and exhibit different temporal coupling dynamics during novelty exploration (SuppFigure 3C). The usage of the same nomenclature (lowG to describe beta2 and lowG) may create difficulties in the characterization of the function behind these different oscillations, which could also be the reason for beta2 being reported only twice in over the past decades (França et al., 2014). Instead of only the band of frequency, in which authors constantly change the frequency range for the same nomenclature, the oscillations ideally should be classified based on different characteristics, from the species been recorded to wave-shape, origin and physiological function (Cole and Voytek, 2017; Tort et al., 2018).

The distinction between beta2 and lowG is also important in the perspective of a complex network involving different brain regions, because beta oscillations are implicated in long-range synchrony between different areas of the brain, a feature not shared with gamma oscillations (Kopell et al., 2000). For the first time, we revealed that during the novelty exploration sessions the HC has a strong coherence in the beta2 frequency band (Figure 3A and B), such coherence is not seen when the animal

never faced the novelty content before (Figure 3C). On top of that, Granger causality revealed that the highest Granger gains comes from HC and PAR cortex towards mPFC in theta, beta2 and lowG frequency band during OF1 exploration, while in the object novelty session the Granger gain comes mostly from HC (Figure 3D and E). Note that during the subsequent familiar exploration sessions the beta2 coherence in all three areas remains strong, probably carrying novelty content information towards the cortices that act like hubs for comparing the familiarity/novelty contents. The coherence and Granger results point to the close communication among the three areas recorded, showing that all three areas communicate via theta and beta2 during novelty and familiarity exploration.

We also have shown that Beta2 has similar transient power dynamics in the mPFC, increasing in the beginning of session and fading towards the end of the session (Figure 4A). Although PAR did not exhibit a statistically significant increase in the beta2 power, similar to HC, the beta2 bursts can be verified in the raw signal of mPFC and PAR channels coherent to other areas or in independent bursts (SuppFigure 3). Lastly, we have shown that similar to HC coupling dynamics, both cortices exhibit strong coupling between theta/midG and theta/lowG during novelty exploration and the same coupling between delta/beta2 exhibited in HC in the first time window that beta2 exhibited higher power (Figure 4B and D), these couple is only verified in during the novelty exploration (Figure 4), but not during familiar exploration (SuppFigure B and C) suggesting that the cortical process of information is mostly done during novelty exploration. Similar coupling was previously reported in the mid-prefrontal cortex during recording in freely behaving rodents (Andino-Pavlovsky et al., 2017) or during learning and working memory (Canolty and Knight, 2010; I.b.h, 2019). However, for the first time we show that the local delta oscillations modulate the beta2 not only in the HC, but also in the PAR and mPFC cortices during novelty exploration.

Together, these results highlight the importance of beta2 oscillations in a larger hippocampal-cortical circuit, suggesting that beta2 is a mechanism for detecting and communicating novelty information among the areas involved in modulating and behavioral adaptation to novelty.

Reference

Andino-Pavlovsky, V., Souza, A.C., Scheffer-Teixeira, R., Tort, A.B.L., Etchenique, R., and Ribeiro, S. (2017). Dopamine Modulates Delta-Gamma Phase-Amplitude Coupling in the Prefrontal Cortex of Behaving Rats. Front. Neural Circuits *11*.

Barnett, L., and Seth, A.K. (2014). The MVGC multivariate Granger causality toolbox: a new approach to Granger-causal inference. J. Neurosci. Methods 223, 50–68.

Benchenane, K., Peyrache, A., Khamassi, M., Tierney, P.L., Gioanni, Y., Battaglia, F.P., and Wiener, S.I. (2010). Coherent Theta Oscillations and Reorganization of Spike Timing in the Hippocampal- Prefrontal Network upon Learning. Neuron 66, 921–936.

Benchenane, K., Tiesinga, P.H., and Battaglia, F.P. (2011). Oscillations in the prefrontal cortex: a gateway to memory and attention. Curr. Opin. Neurobiol. 21, 475–485.

Berke, J.D., Hetrick, V., Breck, J., and Greene, R.W. (2008). Transient 23-30 Hz oscillations in mouse hippocampus during exploration of novel environments. Hippocampus 18, 519–529.

Buzsáki, G., and Draguhn, A. (2004). Neuronal oscillations in cortical networks. Science 304, 1926–1929.

Canolty, R.T., and Knight, R.T. (2010). The functional role of cross-frequency coupling. Trends in Cognitive Sciences 14, 506–515.

de Cheveigné, A., and Arzounian, D. (2015). Scanning for oscillations. J Neural Eng 12, 066020.

Cohen, M.X. (2017). Comparison of linear spatial filters for identifying oscillatory activity in multichannel data. J. Neurosci. Methods 278, 1–12.

Cole, S.R., and Voytek, B. (2017). Brain Oscillations and the Importance of Waveform Shape. Trends in Cognitive Sciences 21, 137–149.

Colgin, L.L. (2015). Theta-gamma coupling in the entorhinal-hippocampal system. Curr. Opin. Neurobiol. 31, 45–50.

Cross, L., Brown, M.W., Aggleton, J.P., and Warburton, E.C. (2013). The medial dorsal thalamic nucleus and the medial prefrontal cortex of the rat function together to support associative recognition and recency but not item recognition. Learn. Mem. 20, 41–50.

Delorme, A., Mullen, T., Kothe, C., Akalin Acar, Z., Bigdely-Shamlo, N., Vankov, A., and Makeig, S. (2011). EEGLAB, SIFT, NFT, BCILAB, and ERICA: New Tools for Advanced EEG Processing. Computational Intelligence and Neuroscience 2011, 1–12.

França, A.S.C., do Nascimento, G.C., Lopes-dos-Santos, V., Muratori, L., Ribeiro, S., Lobão-Soares, B., and Tort, A.B.L. (2014). Beta2 oscillations (23–30 Hz) in the mouse hippocampus during novel object recognition. Eur J Neurosci 40, 3693–3703.

Franca, A.S.C., Hulten, J.A. van, and Cohen, M.X. (2020). Low-cost and versatile electrodes for extracellular chronic recordings in rodents. BioRxiv 2020.02.06.937201.

Fries, P. (2005). A mechanism for cognitive dynamics: neuronal communication through neuronal coherence. Trends in Cognitive Sciences 9, 474–480.

Hasselmo, M.E. (2006). The role of acetylcholine in learning and memory. Current Opinion in Neurobiology 16, 710–715.

Haufe, S., Dähne, S., and Nikulin, V.V. (2014). Dimensionality reduction for the analysis of brain oscillations. Neuroimage 101, 583–597.

Hyafil, A., Giraud, A.-L., Fontolan, L., and Gutkin, B. (2015). Neural Cross-Frequency Coupling: Connecting Architectures, Mechanisms, and Functions. Trends in Neurosciences 38, 725–740.

I.b.h, S. (2019). Gamma band oscillations drives information flow in theta and delta band between hippocampus and medial pre-frontal cortex. BioRxiv 809962.

Kafkas, A., and Montaldi, D. (2018). How do memory systems detect and respond to novelty? Neurosci. Lett. 680, 60–68.

van Kesteren, M.T.R., Ruiter, D.J., Fernández, G., and Henson, R.N. (2012). How schema and novelty augment memory formation. Trends Neurosci. 35, 211–219.

Kitanishi, T., Ujita, S., Fallahnezhad, M., Kitanishi, N., Ikegaya, Y., and Tashiro, A. (2015). Novelty-Induced Phase-Locked Firing to Slow Gamma Oscillations in the Hippocampus: Requirement of Synaptic Plasticity. Neuron 86, 1265–1276.

Kopell, N., Ermentrout, G.B., Whittington, M.A., and Traub, R.D. (2000). Gamma rhythms and beta rhythms have different synchronization properties. PNAS 97, 1867–1872.

de Lima, M.N.M., Presti-Torres, J., Dornelles, A., Siciliani Scalco, F., Roesler, R., Garcia, V.A., and Schröder, N. (2011). Modulatory influence of dopamine receptors on consolidation of object recognition memory. Neurobiology of Learning and Memory 95, 305–310.

Lisman, J.E., and Grace, A.A. (2005). The hippocampal-VTA loop: controlling the entry of information into long-term memory. Neuron 46, 703–713.

Lisman, J.E., and Jensen, O. (2013). The theta-gamma neural code. Neuron 77, 1002–1016.

Lisman, J.E., and Otmakhova, N.A. (2001). Storage, recall, and novelty detection of sequences by the hippocampus: elaborating on the SOCRATIC model to account for normal and aberrant effects of dopamine. Hippocampus 11, 551–568.

Lopes-dos-Santos, V., van de Ven, G.M., Morley, A., Trouche, S., Campo-Urriza, N., and Dupret, D. (2018). Parsing Hippocampal Theta Oscillations by Nested Spectral Components during Spatial Exploration and Memory-Guided Behavior. Neuron 100, 940-952.e7.

Pho, G.N., Goard, M.J., Woodson, J., Crawford, B., and Sur, M. (2018). Task-dependent representations of stimulus and choice in mouse parietal cortex. Nature Communications 9, 1–16.

Preston, A.R., and Eichenbaum, H. (2013). Interplay of hippocampus and prefrontal cortex in memory. Curr Biol 23, R764–R773.

Sigurdsson, T., Stark, K.L., Karayiorgou, M., Gogos, J.A., and Gordon, J.A. (2010). Impaired hippocampal–prefrontal synchrony in a genetic mouse model of schizophrenia. Nature 464, 763–767.

Spellman, T., Rigotti, M., Ahmari, S.E., Fusi, S., Gogos, J.A., and Gordon, J.A. (2015). Hippocampal–prefrontal input supports spatial encoding in working memory. Nature 522, 309–314.

Tort, A.B.L., Kramer, M.A., Thorn, C., Gibson, D.J., Kubota, Y., Graybiel, A.M., and Kopell, N.J. (2008). Dynamic cross-frequency couplings of local field potential oscillations in rat striatum and hippocampus during performance of a T-maze task. Proc. Natl. Acad. Sci. U.S.A. 105, 20517–20522.

Tort, A.B.L., Komorowski, R.W., Manns, J.R., Kopell, N.J., and Eichenbaum, H. (2009). Theta–gamma coupling increases during the learning of item–context associations. PNAS 106, 20942–20947.

Tort, A.B.L., Ponsel, S., Jessberger, J., Yanovsky, Y., Brankačk, J., and Draguhn, A. (2018). Parallel detection of theta and respiration-coupled oscillations throughout the mouse brain. Scientific Reports 8, 1–14.

Vinck, M., Oostenveld, R., van Wingerden, M., Battaglia, F., and Pennartz, C.M.A. (2011). An improved index of phase-synchronization for electrophysiological data in the presence of volume-conduction, noise and sample-size bias. NeuroImage 55, 1548–1565.

Zheng, C., Bieri, K.W., Hwaun, E., and Colgin, L.L. (2016). Fast Gamma Rhythms in the Hippocampus Promote Encoding of Novel Object–Place Pairings. ENeuro 3.

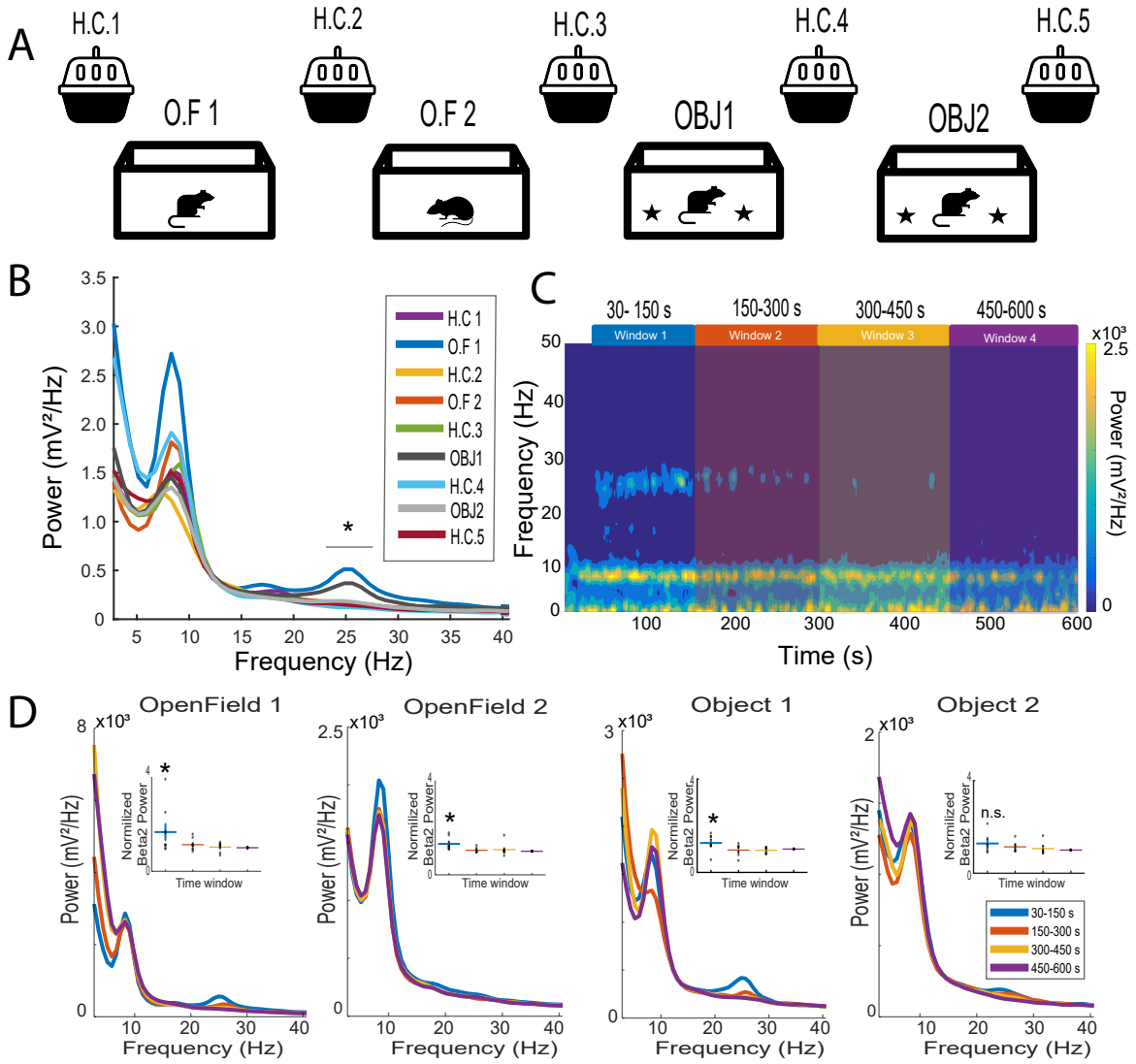
A
H.C.1
O.F 1
H.C.2
O.F 2
H.C.3
OBJ1
H.C.4
OBJ2
H.C.5
B
Power (mV²/Hz)
Frequency (Hz)
H.C 1
O.F 1
H.C.2
O.F 2
H.C.3
OBJ1
H.C.4
OBJ2
H.C.5
C
30- 150 s
150-300 s
300-450 s
450-600 s
Window 1
Window 2
Window 3
Window 4
Frequency (Hz)
Time (s)
x10³
Power (mV²/Hz)
D
OpenField 1
OpenField 2
Object 1
Object 2
Power (mV²/Hz)
Frequency (Hz)
Normilized Beta2 Power
Time window
n.s.
30-150 s
150-300 s
300-450 s
450-600 s

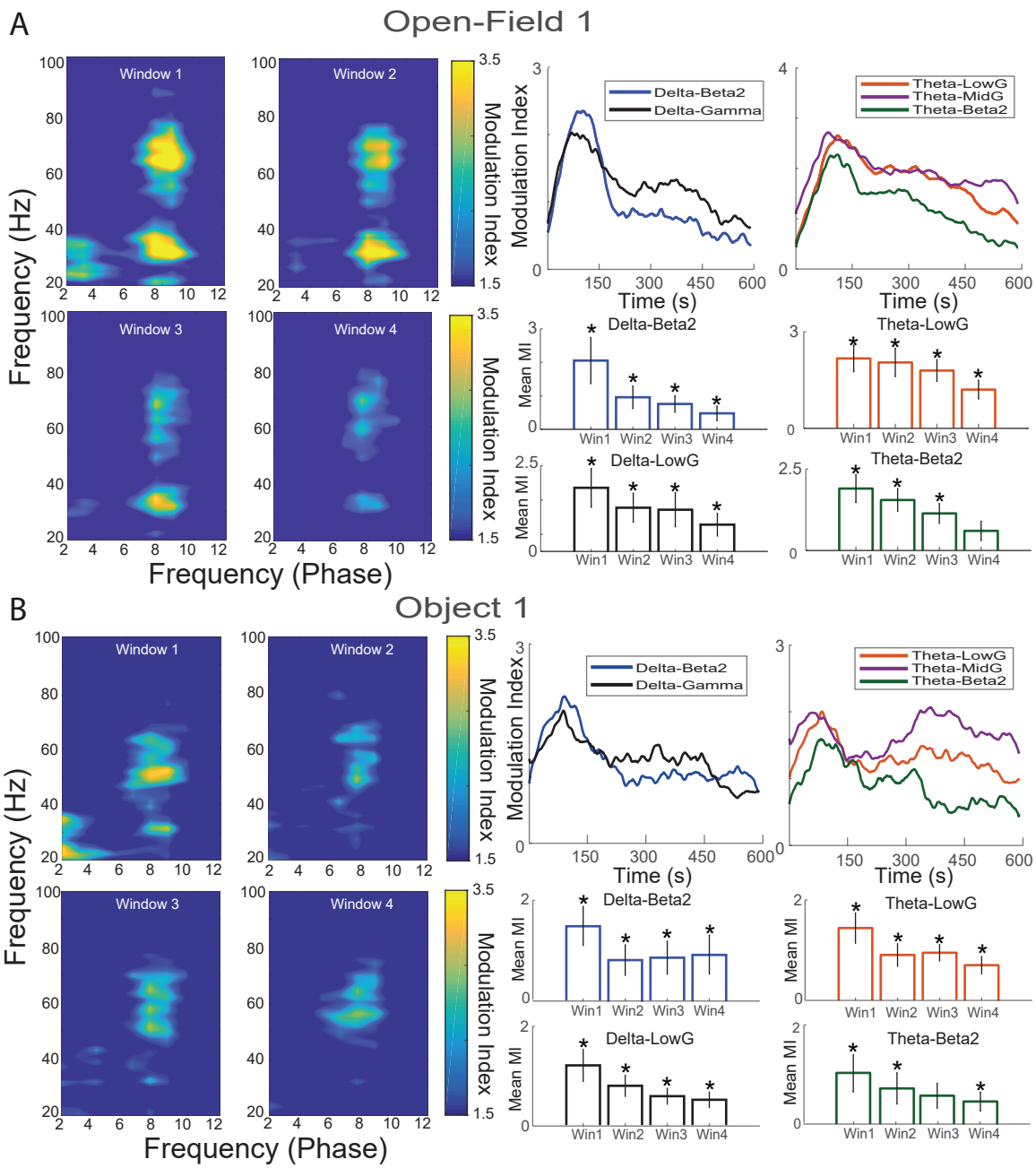
A
Open-Field 1
Window 1
Window 2
Window 3
Window 4
Frequency (Hz)
Frequency (Phase)
Modulation Index
Delta-Beta2
Delta-Gamma
Theta-LowG
Theta-MidG
Theta-Beta2
Time (s)
Mean MI
Delta-LowG
Win1
Win2
Win3
Win4
B
Object 1

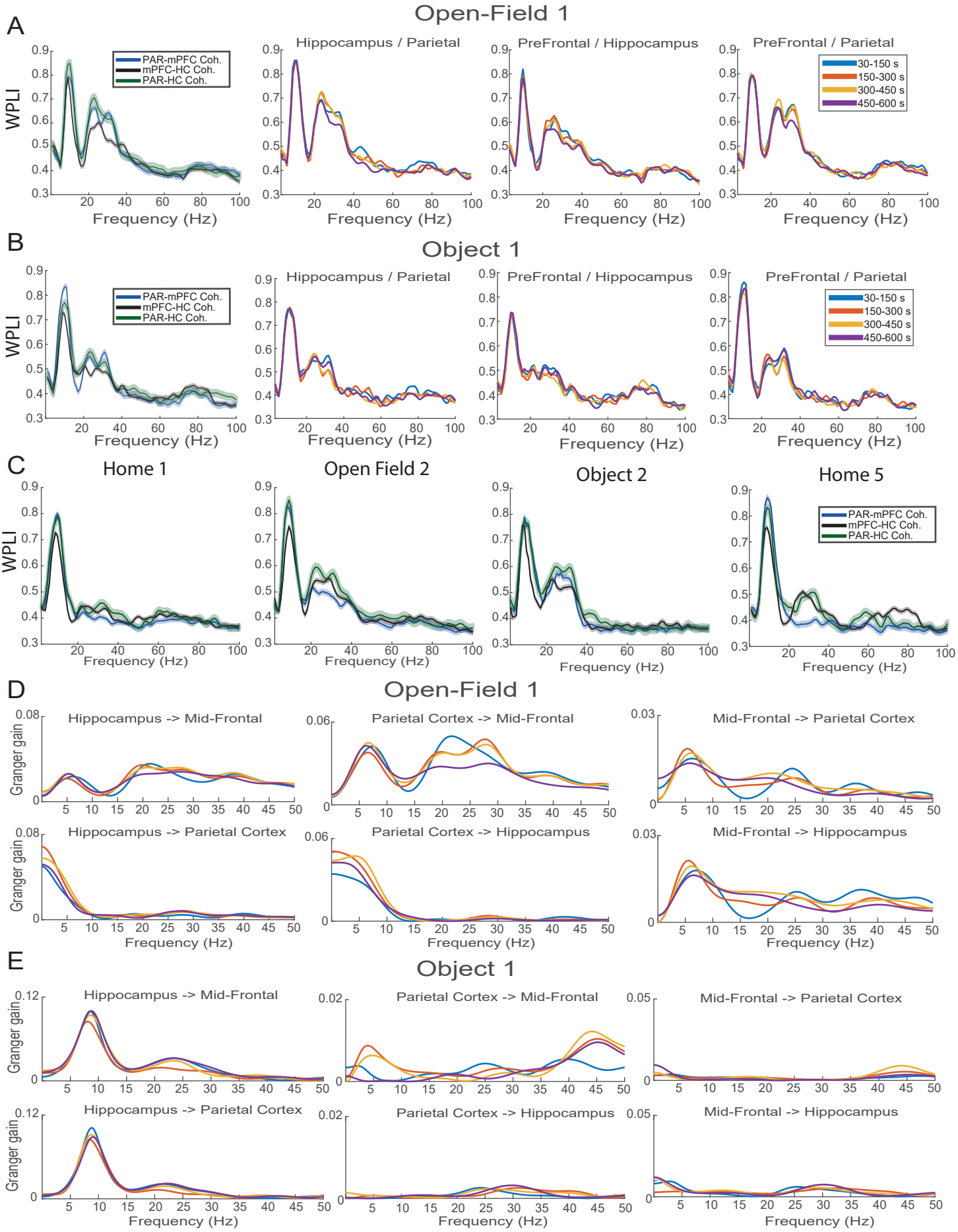
A
Open-Field 1
WPLI
PAR-mPFC Coh.
mPFC-HC Coh.
PAR-HC Coh.
Hippocampus / Parietal
PreFrontal / Hippocampus
PreFrontal / Parietal
30-150 s
150-300 s
300-450 s
450-600 s
Frequency (Hz)
B
Object 1
C
Home 1
Open Field 2
Object 2
Home 5
D
Open-Field 1
Granger gain
Hippocampus -> Mid-Frontal
Parietal Cortex -> Mid-Frontal
Mid-Frontal -> Parietal Cortex
Hippocampus -> Parietal Cortex
Parietal Cortex -> Hippocampus
Mid-Frontal -> Hippocampus
E
Object 1

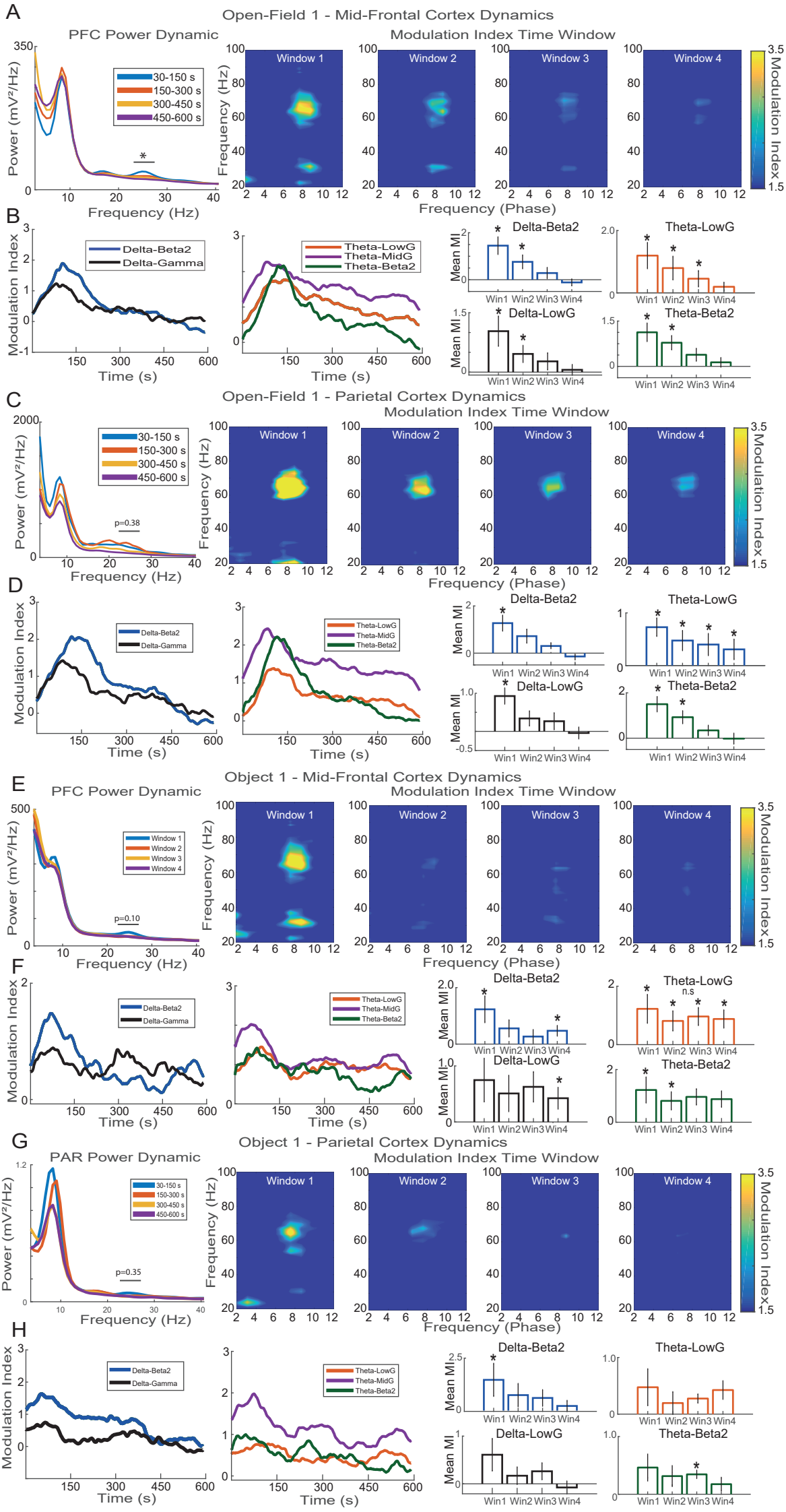
A
Open-Field 1 - Mid-Frontal Cortex Dynamics
PFC Power Dynamic
Modulation Index Time Window
Power (mV²/Hz)
Frequency (Hz)
30-150 s
150-300 s
300-450 s
450-600 s
Window 1
Window 2
Window 3
Window 4
Frequency (Hz)
Frequency (Phase)
Modulation Index
B
Modulation Index
Time (s)
Delta-Beta2
Delta-Gamma
Theta-LowG
Theta-MidG
Theta-Beta2
Mean MI
Delta-LowG
Win1 Win2 Win3 Win4
C
Open-Field 1 - Parietal Cortex Dynamics
p=0.38
D
E
Object 1 - Mid-Frontal Cortex Dynamics
p=0.10
F
n.s
G
Object 1 - Parietal Cortex Dynamics
PAR Power Dynamic
p=0.35
H